A New Class of Polyintercalating Molecules

R. Scott Lokey,[†] Yan Kwok,[‡] Vladimir Guelev,[†] Christopher J. Pursell,[§] Laurence H. Hurley,[‡] and Brent L. Iverson*,[†]

Contribution from the Departments of Chemistry, Biochemistry, and Pharmacy, The University of Texas at Austin, Austin, Texas 78712, and Department of Chemistry, Trinity University, San Antonio, Texas 78212

Received February 25, 1997[⊗]

Abstract: We have synthesized a series of polyintercalating compounds, including the first known tetraintercalator, based on the 1,4,5,8-naphthalenetetracarboxylic diimide chromophore. The chromophores are attached in a head-to-tail arrangement by peptide linkers and are synthesized by standard solid phase peptide synthesis methods. We report evidence, based on UV−visible spectroscopy and viscometry, that the compounds are fully intercalated upon binding to double-stranded DNA. Using DNAse I footprinting experiments, the bisintercalator **2** was found to bind to DNA in a cooperative manner. The footprinting results as well as association and dissociation kinetics data reveal that the compounds exhibit a tremendous preference for GC over AT sequences. A mode of binding is proposed in which the compounds intercalate completely from the major groove, and not in a threading manner as may be suggested by their structures. A kinetic scheme is proposed that takes into account the observed cooperativity and fits the data for the dissociations of the polyintercalators from poly(dAdT), although a similar scheme could not adequately model their dissociations from poly(dGdC) or from calf thymus DNA.

Introduction

Numerous compounds, including some clinically used chemotherapeutic agents, interact with DNA by intercalating one or more aromatic groups between base pairs of the double helix. Whereas initial studies focused on molecules with a single intercalating moiety,[1,2] the promise of improved antitumor activity[3−7] and/or sequence specificity[8−10] has led researchers to investigate compounds that contain more than one intercalating group.[11−15] Efforts to extend the interaction beyond bisintercalation, however, have met with relatively few successes.[3,12,16−19] Of the known trisintercalators, most have reported association constants within an order of magnitude of their bisintercalating counterparts; one noteworthy exception is a polyamine-linked triacridine synthesized by Laugâa and coworkers[20] that exhibited an unusually high binding affinity for double-stranded DNA ($K_{app} = 10^{14}$ M^{-1}).

The propensity of a molecule to intercalate two or more groups simultaneously appears to be dependent on both the length and composition of the linking backbone.[3,11,16] The traditional polyintercalating design in which the aromatic units are connected in parallel along a contiguous linker may restrict polyintercalation due to unfavorable distortions in the backbone. Takenaka *et al.*[19] reported a different design in which three acridine units were linked in series, like beads on a string. For these trisintercalating molecules a "threading" type of binding mode was proposed similar to the mono-[21,22] and bisintercalators[23,24] previously known to extend into both grooves of DNA simultaneously. We now report the solid phase synthesis and DNA-binding properties of a new series of polyintercalators, including what is to the best or our knowledge the first known tetraintercalating molecule, in which the aromatic groups are connected in series. These polyintercalators comprise a new class of DNA-binding molecules in which properties such as

* To whom correspondence should be addressed.
† Departments of Chemistry and Biochemistry, The University of Texas at Austin.
‡ Department of Pharmacy, The University of Texas at Austin.
§ Trinity University.
⊗ Abstract published in *Advance ACS Abstracts,* July 1, 1997.

(1) Lerman, J. S. *J. Mol. Biol.* **1961**, *3*, 18−30.
(2) Wilson, W. D.; Jones, R. L. *Adv. Pharm. Chemother.* **1981**, *18*, 177−222.
(3) Wakelin, L. P. G. *Med. Res. Rev.* **1986**, *6*, 275−340.
(4) Chaires, J. B.; Leng, F.; Przewloka, T.; Fokt, I.; Ling, Y. H.; Perez-Soler, R.; Priebe, W. *J. Med. Chem.* **1997**, *40,* 261−266.
(5) Waring, M. J. In Molecular Aspects of Anticancer Drug-DNA Interactions; Neidle, S., Waring, M. J., Eds.; CRC: Boca Raton, FL, 1993; Vol 1, Chapter 7.
(6) Bosquet, P. F.; Braña, M. F.; Conlon, D.; Fitzgerald, K. M.; Perron, D.; Cocchiaro, C.; Miller, R.; Moran, M.; George, J.; Quian, X.-D.; Keilhauer, G.; Romerdahl, C. A. *Cancer Res.* **1995**, *55*, 1176−1180.
(7) McRipley, R. J.; Burns-Horwitz, P. E.; Czerniak, P. M.; Diamond, R. J.; Diamond, M. A.; Miller, J. L. D.; Page, R. J.; Dexter, D. L.; Chen, S.-F.; Sun, J.-H.; Behrens, C. H.; Seitz, S. P.; Gross, J. L. *Cancer Res.* **1994**, *54*, 159−164.
(8) Waring, M. J.; Fox, K. R. *Molecular Aspects of Anticancer Drug Action*; Macmillan: London, 1983.
(9) Delepiene, M.; Milhe, C.; Namane, A.; Dinh, T. H.; Roques, B. P. *Biopolymers* **1991**, *31*, 331−353.
(10) Bailly, C.; Braña, M.; Waring, M. J. *Eur. J. Biochem.* **1996**, *240*, 195−208.
(11) Denny, W. A.; Atwell, G. J.; Willmott, G. A.; Wakelin, L. P. G. *Biophys. Chem.* **1985**, *22*, 17−26.
(12) Wirth, M.; Ole, B.; Torben, K.; Nielsen, P.; Norden, B. J. *J. Am. Chem. Soc.* **1988**, *110*, 932−934.
(13) Atwell, G. J.; Leupin, W.; Twigden, S. J.; Denny, W. F. *J. Am. Chem. Soc.* **1983**, *105*, 2913−2914.
(14) Hansen, J. B.; Koch, T.; Buchardt, O.; Nielsen, P. E.; Wirth, M.; Norden, B. *Biochemistry* **1983**, *22*, 4878−4886.
(15) Denny, W. A. In *Cancer Chemotherapeutic Agents*; Foye, W. O., Ed.; American Chemical Society: Washington DC, 1995; pp 218−239.
(16) Gaugain, B.; Markovits, J.; Le Pecq, J.-B.; Roques, B. P. *FEBS Lett.* **1984**, *169*, 123−126.
(17) Atwell, G. J.; Baguley, B. G.; Wilmanska, D.; Denny, W. A. *J. Med. Chem.* **1986**, *29*, 69−74.
(18) Hansen, J. B.; Koch, T.; Buchardt, O.; Nielsen, P. E.; Nordén, B.; Wirth, M. *J. Chem. Soc., Chem. Commun.* **1984**, 509−511.
(19) Takenaka, S.; Nishira, S.; Tahara, K.; Kondo, H.; Takagi, M. *Supramol. Chem.* **1993**, *2*, 41−46.
(20) Laugâa, P.; Markovits, J.; Delbarre, A.; Le Pecq, J.-B.; Roques, B. P. *Biochemistry* **1985**, *24*, 5567−5575.
(21) Yen, S.; Gabbay, E. J.; Wilson, D. W. *Biochemistry* **1982**, *21*, 2070−2076.
(22) Williams, L. D.; Egli, M.; Gao, Q.; Bash, P.; van der Marel, G.; van Boom, J. H.; Rich, A.; Frederick, C. A. *Proc. Natl. Acad. Sci. U.S.A.* **1990**, *87*, 2225−2229.
(23) Veal, J. M.; Li, Y.; Zimmerman, S. C.; Lamberson, C. R.; Cory, M.; Zon, G.; Wilson, W. D. *Biochemistry* **1990**, *29*, 10918−10927.
(24) Zimmerman, S. C.; Lamberson, C. R.; Cory, M.; Fairley, T. A. *J. Am. Chem. Soc.* **1989**, *111*, 6805−6809.

S0002-7863(97)00610-0 CCC: $14.00

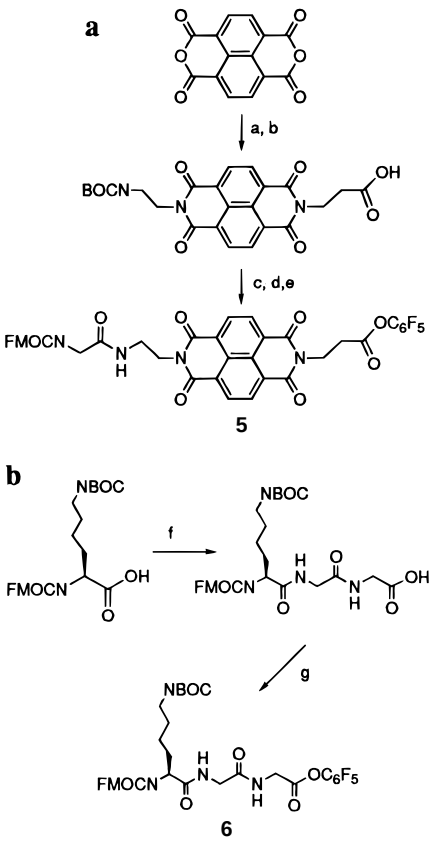

Figure 1. Synthesis of diimide amino acid precursor. Reagents: (a) β-alanine benzyl ester *p*-toluene sulfonate salt, $BOCN(CH_2)_2NH_2$, *i*-Pr_2-NEt; (b) H_2, Pd/C; (c) TFA/CH_2Cl_2; (d) FMOC-Gly-OC_6F_5, HOBT, 2,6-lutidine; (e) pentafluorophenol, DCC; (f) diglycine (TEA salt), sulfo-NHS, EDC; (g) pentafluorophenol, DCC.

sequence specificity and cell permeability can be explored in a general way using combinatorial methods and/or rational design to change the sequence of the linker segments.

Results

Synthesis. Our polyintercalating molecules are based on a modification of the design we reported previously for the construction of so-called "aedamers", synthetic molecules designed to fold into an abiotic secondary structure.[25] The design utilizes 1,4,5,8-naphthalenetetracarboxylic diimide, an electron-deficient aromatic group that has been shown previously to intercalate into double-stranded DNA.[21] Molecular dynamics simulations using a flexible peptide backbone on a bisintercalated DNA template[26] predicted that a four amino acid segment between diimide moieties would have the optimum combination of length and flexibility to span two base pairs, allowing polyintercalation in accord with the general principle of nearest neighbor exclusion. One lysine residue was placed on each segment to provide electrostatic attraction to the DNA. The amino acid building blocks **5** and **6** were synthesized (Figure 1), and compounds **1**−**4** were constructed using standard solid phase peptide synthesis (SPPS) methodology[27] (Figure 2). A number of different studies were carried out to investigate the DNA-binding behavior of the predicted polyintercalators **1**−**4**.

Hypochromism. In aqueous buffer, the diimide chromophores of compound **1**, and compounds **2**−**4**, give rise to absorbance maxima at 382 and 384 nm, respectively. In the absence of DNA, the molar extinction coefficients of **2**−**4** at 384 nm, divided by the number of chromophores in each molecule, are significantly less than the extinction coefficient of **1** at that wavelength (Table 1). In 2% SDS solution, however, the absorbance spectra of **2**−**4** are simple multiples of the spectrum of **1** (Table 1), both in terms of extinction coefficient and lineshape.

All of the polyintercalators show, in accord with previous studies using the same chromophore,[21] significant hypochromism upon binding to double-stranded DNA (Supporting Information). This absorbance change in the ultraviolet spectrum upon intercalation was used to study the equilibrium and kinetic aspects of the interactions of compounds **1**−**4** with DNA.

Binding Studies. The binding isotherm between **1** and CT DNA was determined spectrophotometrically and fit according to the McGee−von Hippel equation.[28] A value of 1.4×10^4 M^{-1} was obtained for K_{eq}, and the expected value[29] of 2.0 base pairs was obtained for *n*, the binding site size (Figure 3). Direct equilibrium analyses could not be carried out with **2**−**4**, because free ligand could not be detected in a concentration regime low enough to evaluate their association constants ($>10^7$ as estimated from the DNAse I footprinting results, *vide infra*).

Unwinding Studies. The helix extension parameter, which is a measure of the lengthening of linear fragments of double stranded CT DNA, was determined for each compound visco-

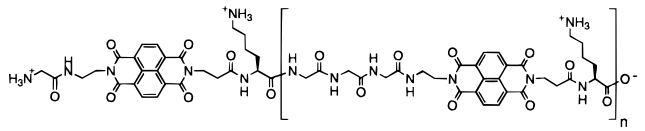

Figure 2. Polyintercalators **1** ($n = 0$), **2** ($n = 1$), **3** ($n = 2$), and **4** ($n = 3$), synthesized using standard solid phase peptide synthesis techniques from monomers **5** and **6**.

Table 1. Spectroscopic and Viscometric Data for Compounds **1**−**4**

compd	ϵ_F[a]	ϵ_B[b]	ϵ_{Det}[c]	ϕ[d] (deg)	m[e]
1	20 000	10 400	23 400	12	0.41
2	27 400	20 100	44 000	24	0.84
3	39 200	27 700	74 600	37	1.4
4	51 300	39 500	96 000	48	1.9

[a] Extinction coefficients at 386 nm, determined in 10 mM TRIS buffer with 1 mM EDTA and 50 mM NaCl. [b] Extinction coefficients (386 nm) in same buffer containing large excess of CT DNA. [c] Extinction coefficients (386 nm) in 2% SDS. [d] Unwinding angles. [e] Helix extension parameters.

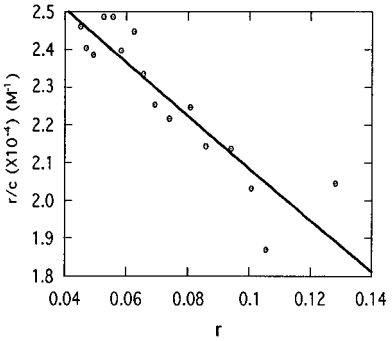

Figure 3. Binding isotherm of **1** and calf thymus DNA, determined spectrophotometrically using the change in absorbance of **1** at 386 nm upon addition of DNA. The data were fit to the McGee−von Hippel equation,[28] where r = the concentration of bound ligand divided by the total concentration of DNA, and c = the concentration of free ligand.

(25) Lokey, R. S.; Iverson, B. L. *Nature* **1995**, 375.
(26) Peek, M. E.; Lipscomb, L. A.; Bertrand, J. A.; Gao, Q.; Roques, B. P.; Garbay-Jaureguiberry, C.; Williams, L. D. *Biochemistry* **1994**, *33*, 3794−3800.
(27) Atherton, E.; Shepard, R. C. *Solid Phase Peptide Synthesis*; IRL: Oxford, 1989.
(28) McGhee, J. D.; von Hippel, P. H. *J. Mol. Biol.* **1974**, *86*, 469−489.
(29) Crothers, D. M. *Biopolymers* **1968**, *6*, 575.
(30) Cohen, G.; Eisenberg, H. *Biopolymers* **1969**, *8*, 45−49.

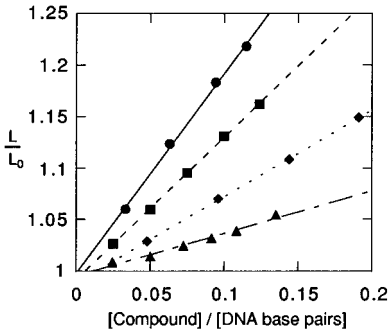

Figure 4. Viscometric titrations of **1** (▲); **2** (♦); **3** (■); and **4** (●) with sonicated calf thymus DNA, carried out in TE buffer (10 mM Tris, 1 mM EDTA) with 50 mM NaCl at 20 °C. Since the monomer was only partially bound at the concentrations used in the viscosity experiment, the [compound]/[DNA base pairs] values were corrected based on the known association constant ($K_a = 1.0 \times 10^5\ M^{-1}$) obtained from the spectrophotometric titration of **1** with calf thymus DNA.

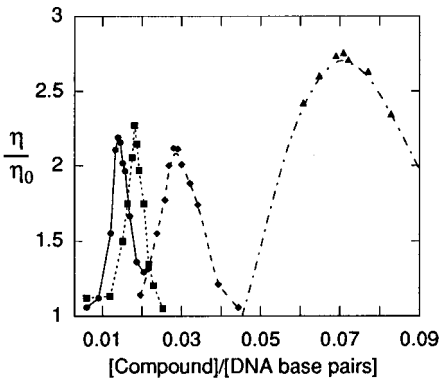

Figure 5. Unwinding of closed circular supercoiled plasmid DNA by compounds **1** (▲); **2** (♦); **3** (■); and **4** (●). For monomer **1**, equivalence point ratios at three different DNA concentrations were plotted vs the concentration of DNA and the true equivalence point was extrapolated according to Vinograd *et al.*[31] Unwinding angles were calculated based on an unwinding angle for ethidium bromide of 26°.

metrically.[30] As shown in Figure 4, the slopes (*m*) increase in increments according to the number of diimide groups per molecule. The unwinding angles for compounds **1**−**4** were determined using standard viscometric methods[31] with closed circular supercoiled plasmid (CCS) DNA (Figure 5). As with the helix extension parameters, the unwinding angles for **2**−**4** are multiples of that found for **1**.

Kinetics Studies. To investigate the dynamics of the interactions of **1**−**4** with DNA, association and dissociation rates were determined for CT DNA, poly(dAdT), and poly(dGdC) (Tables 2 and 3, respectively). The association rates and monomer dissociation rates required stopped-flow techniques, while the slower off-rates for compounds **2**−**4** were measured using a standard spectrophotometer. All dissociation rate measurements required the presence of 2% SDS in the buffer to sequester the dissociated intercalators. Control studies revealed that compounds **1**−**4** did not reassociate with the nucleic acids in 2% SDS, but at lower SDS concentrations, reassociation was observed.

For all of the association profiles, calculated fits represent the minimum number of exponentials required to give purely random residuals. Most of the dissociation profiles were also adequately described by up to three exponentials (the kinetic traces are available as Supporting Information). The dissociation profiles of compounds **2**−**4** from CT DNA, however, were too complex to be fit even to a triexponential decay process, and reproducibly nonrandom residuals were obtained in each of these cases. This complexity is not unexpected considering the sequence heterogeneity of natural DNA and the large number of potential binding sites. Compound **1**, with only one diimide

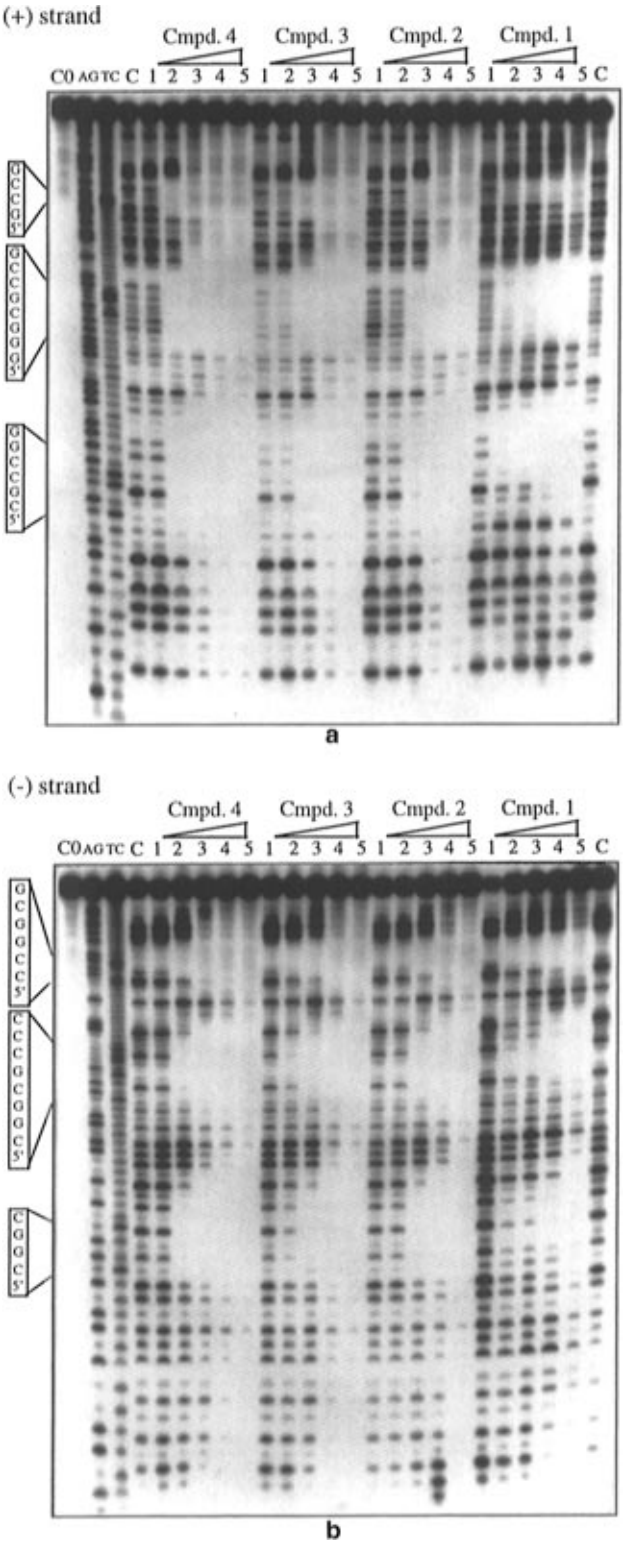

Figure 6. DNAse I footprinting analysis of 78-mer DNA with the "+" (a) and "−" (b) strands labeled on its 5′ end, in the presence of compounds **1**−**4**. Lanes labeled AG and TC represent the purine- and pyrimidine-specific sequencing reactions. Lane C0 contains DNA without DNAse I. Lane C contains DNA with DNAse I but no compound. For compound **1**, lanes 1−5 contain 0.5, 5, 50, 100, and 500 μM compound, respectively. For compounds **2**−**4**, lanes 1−5 contain 62.5, 125, 250, 500, and 1000 nM compound, respectively.

(31) Revét, B. M. J.; Schmir, M.; Vinograd, J. *Nature New Biol*. **1971**, *229*, 10−13.

unit, shows distinct kinetic behavior that is generally faster, both in terms of on- and off-rates, and less complex than the polyintercalators **2**−**4**.

The kinetic data reveal that **1**−**4** exhibit a dramatic preference for poly(dGdC) over poly(dAdT), reflected primarily in their dissociation rates. While the dissociations of compounds **2**−**4** from poly(dAdT) are essentially complete within 200 s, the longest (and most predominant) component of their dissociations from poly(dGdC) has a half-life of *at least* 48 h. Interestingly, compounds **2**−**4** have virtually identical dissociation rate profiles, in terms of their time constants and relative amplitudes. The slowest components for the dissociation of **2**−**4** from poly(dGdC) could not be determined with accuracy because of baseline drift and some sample precipitation over the long period required to observe complete dissociation of the complex. Experiments were performed in which the compounds were mixed with poly(dGdC) dissolved in 2% SDS, and in no case could reassociation be observed, even over a period of several days. This indicates that the dissociations from poly(dGdC) go to completion and not to some partially bound equilibrium state. To fit the dissociation curves for poly(dGdC), the asymptote representing complete dissociation was set as a constant according to the known extinction coefficients of the compounds in 2% SDS.

DNAse I Footprinting. A synthetic oligonucleotide duplex was used for the footprinting studies that contained three GC sites of four, six, and eight base pairs in length, separated by stretches of AT. The footprinting gels (Figure 6a,b) reveal the predicted preferential binding at the GC tracts for all the molecules including the monomer **1**. For each of the polyintercalators **2**−**4**, all three of the GC sites became occupied simultaneously within a narrow range of polyintercalator concentration. The dimer and tetramer show identical footprinting patterns; the only difference between corresponding lanes is that a 2-fold higher concentration of **2** is required to produce the same footprint made by **4**. Although the footprint of the trimer is similar to those of the dimer and tetramer, there is an important difference: Whereas the dimer apparently binds cooperatively to the GC sites (see discussion section below), the footprint of the trimer appears to increase gradually in size as a function of concentration. For example, the trimer displays a significantly smaller footprint at 125 than at 250 nM, while the dimer appears to be completely unbound at 125 nM and completely bound to the GC sites at 250 nM.

Chemical Footprinting. Chemical footprinting methods are often employed to elucidate the groove and sequence preferences of DNA-binding molecules. Using Fe-EDTA, which cleaves DNA largely via the minor groove, and dimethyl sulfate (DMS), which alkylates the N7 position of guanine and causes cleavage via the major groove, footprinting experiments were carried out with the same oligonucleotides used in the DNAse I studies. Studies were performed under conditions in which **1**−**4** are known to be bound, but in no case was protection from cleavage by either chemical reagent observed. On the contrary, in the DMS experiments *enhancement* of methylation-induced cleavage was seen at most of the bound guanosine positions (data not shown), possibly indicative of distortion at the bound GC sequences.

Discussion

Degree of Intercalation. In the absence of DNA, compounds **2**−**4** give rise to absorbance spectra lower in intensity and different in shape from what would be expected by simply multiplying the absorbance spectrum of **1** by the number of chromophores present in each molecule. This, and the significant upfield shift of the diimide hydrogens in the ^{1}H NMR spectra of **2**−**4** relative to **1**, is indicative of intramolecular association of the hydrophobic diimide groups in aqueous solution. In 2% SDS solution, however, the absorbance spectra of **2**−**4** are in fact simple multiples of the spectrum of **1** (Table 1), both in terms of extinction coefficient and lineshape. Presumably, the SDS disrupts the hydrophobic interactions that are responsible for the stacked conformations in aqueous buffer.

Table 2. Association Rates

	1[a]		**2**		**3**		**4**	
DNA type	k^b (s^{-1})	A^c (%)	k (s^{-1})	A (%)	k (s^{-1})	A (%)	k (s^{-1})	A (%)
poly(dAdT)	12.0	100	40.1	33	41.9	38	28.4	32
			4.1	48	4.9	44	4.8	42
			0.90	19	0.99	18	1.2	26
poly(dGdC)	29.2	22	6.6	37	5.7	40	4.7	49
	8.3	78	1.3	25	0.70	38	0.60	27
			0.28	38	0.083	22	0.094	24
CT DNA	38.5	42	3.9	36	9.6	23	8.4	29
	9.7	43	1.2	31	2.1	41	1.6	38
	0.78	15	0.25	43	0.28	36	0.28	33

While in general it may not be appropriate to deduce the degree of intercalation of a compound based on its absorbance spectrum, trends in extinction coefficients (as well as other physical properties, such as unwinding parameters) in a homologous series of compounds contain information when isolated measurements for any one compound would not. Such is the case for the series **1**−**4** bound to DNA. For example, if all of the chromophores in a homologous series such as **1**−**4** are intercalated, one would expect (in the absence of significant perturbations between neighboring intercalated groups) the absorption spectra of their DNA-bound states to follow the simple equation

$$\epsilon_{\mathbf{n}(\text{bound})} = n\epsilon_{\mathbf{1}(\text{bound})}$$

where $\epsilon_{\mathbf{1}(\text{bound})}$ is the extinction coefficient of the monomer bound to DNA and $\epsilon_{\mathbf{n}(\text{bound})}$ is the extinction coefficient of compound **n**, with n chromophores, bound to DNA. This is the case for compounds **1**−**4**, as shown in Table 1. In this system, the analysis is particularly sensitive to the existence of unbound chromophores because the extinction coefficient of the unbound monomer is over 2-fold higher than that of the bound monomer. Any diimide groups remaining free in solution would be expected to contribute a larger absorbance and thus increase the value of $\epsilon_{\mathbf{n}(\text{bound})}$ above that observed.

The helix extension parameters and unwinding angles of **2**−**4** are also simply multiples of the values measured for compound **1**, suggesting that all of the molecules have each chromophore intercalated. It is worth noting that the values for the compound **1**, namely 0.41 and 12° for the helix extension parameter and unwinding angle, respectively, are somewhat lower than what has been observed for some intercalators.[30] Nevertheless, our values fall within the range observed for other intercalators that contain the same diimide chromophore.[21] Thus, it appears that the peptide tether has little effect on the degree to which each intercalating moiety lengthens double-stranded DNA. Taken together, the above spectroscopic and unwinding data indicates full intercalation of compounds **2**−**4**. To the best of our knowledge, this represents the first example, despite at least one published attempt,[12] of tetraintercalation by a single molecule.

Kinetics. In general, the similarity in the rates of association of **2**−**4** with a given type of DNA (Table 2) can be related to a rate-determining preassociation step that is independent of the specific DNA−ligand interactions. For example, such similarity

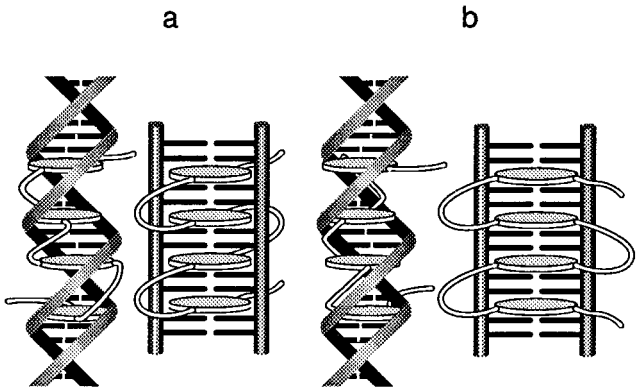

Figure 7. Schematic representation of the binding of tetraintercalator **4** to double stranded DNA by **A** weaving into and out of the double helix such that the linkers reside in both grooves or by **B** intercalation solely from one side of the double helix.

in on-rates was observed among a series of mono-, bis-, and trisacridines with poly(dAdT) and was attributed to rate-limiting desolvation of both the ligand and the DNA to form a preassociation complex.[20,33] Since polyintercalators **2**−**4** exhibit a significant degree of self-stacking in aqueous solution, it is also possible that a slow unstacking step, likely intramolecular but possibly having some intermolecular components at higher concentrations, is required before these molecules are able to intercalate. The monomer, which is not significantly aggregated under the conditions of the association experiments (*vide supra*), displays significantly faster association rates than **2**−**4** for the different DNAs, consistent with the above idea.

Cooperativity. A synthetic oligonucleotide duplex was used for the footprinting studies that contained three GC sites of four, six, and eight basepairs in length, separated by stretches of AT. The footprinting gels (Figure 6a,b) reveal the predicted preferential binding at the GC tracts for all the molecules including the monomer **1**. For each of the polyintercalators **2**−**4**, all three of the GC sites became occupied simultaneously within a very narrow range of polyintercalator concentration. The dimer and tetramer show identical footprinting patterns; the only difference between corresponding lanes is that a 2-fold higher concentration of **2** is required to produce the same footprint made by **4**. Importantly, at no concentration is any footprint smaller than nine basepairs observed with **2** (or **4**). That is, the cooperative binding of two molecules of **2** simultaneously is more favorable than binding of a single molecule of **2**, thereby explaining the nine basepair footprint *even at the four basepair GC site*. Cooperative binding behavior has recently been reported for the bisintercalating drug echinomycin.[32]

Binding Modes. The DNA-bound state of a tetraintercalating polydiimide such as **4** can be represented by at least two distinct schematic models (Figure 7). Wilson *et al*. observed the intercalation of several compounds containing the 1,4,5,8-naphthalenetetracarboxylic diimide moiety with bulky groups such as adamantyl attached at both of the nitrogen atoms.[21] These authors proposed that in order to intercalate, at least one of the bulky groups must pass through the double helix, invoking a dynamic model of DNA that allows for transient DNA breathing, even at temperatures well below its melting temperature. This type of "threading" intercalation has been attributed to other DNA-binding compounds, namely the drug nogalamycin,[22,34] and Takenaka *et al*.[19] reported a trisintercalating molecule that was proposed to bind in a threading manner. Applying this reasoning to compounds **3** and **4** of our system results in a structure, referred to here as model **A**, in which the aromatic groups thread through the double helix such that their linker segments reside in the major and minor grooves in an alternating fashion (Figure 7a).

An alternative possibility for the bound structure, referred to here as model **B**, is one in which the diimide groups intercalate into double-stranded DNA "edge-on", while the linker segments reside entirely within the same DNA groove (Figure 7b). The helical twist of the DNA duplex could allow for considerable intercalation of the diimides within the major groove, while still providing enough space for the linker chains to extend from each end of the diimide. Although the chemical footprinting results were inconclusive regarding the groove preference of compounds **2**−**4**, we consider similar binding in the smaller minor groove unlikely on steric grounds. Moreover, a recent report by Waring *et al*.[10] on LU799553, a naphthalimide bisintercalator, indicates that the naphthalimide moiety in this molecule probably intercalates via the major groove of DNA. Some hybrid of modes **A** and **B** is also possible with **3** and **4**. In the absence of definitive structural data from either NMR spectroscopy or X-ray crystallography (these methods have yielded little information to date), we have relied on more indirect routes to discern the binding modes of compounds **1**−**4**. As described below, based primarily on kinetic evidence, we conclude that of the two model **B** is more consistent with the available data.

All components of the stopped-flow association kinetics of **1**−**4** with poly(dGdC) are several times slower than those for poly(dAdT), implying that transient breathing of the double helix (an event that is about 25 times more likely for an AT than a GC base pair)[35,36] has an influence on the rates of association. This would tend to favor model **A**; indeed, Fox and Waring observe a similar trend in the association of the threading intercalator nogalamycin,[34] certain components of which they ascribe to a rate-determining DNA breathing step. If, however, model **A** is correct, then one would not expect such similar kinetic behavior among all of the polyintercalating species **2**−**4**. Relative to the bisintercalator **2**, the tris- and tetraintercalators would require extra, presumably rate-limiting, steps to thread into, and out of, the double helix. On the other hand, if DNA binding proceeded according to model **B**, the accessibility of the major groove would be similar to all intercalating units in the ligand and could result in the observed similar rate profiles for the polyintercalators.

Specifically, according to model **A**, one would expect **3** and **4** to display significantly slower off-rates compared with **2**. A salient feature of the dissociation data is that, within a given type of DNA, compounds **2**−**4** display remarkably *similar* kinetic behavior. This includes all of the key parameters of the fits, including the number of components observed, the relative extent of each component, and the magnitudes of the derived constants. No reasonable mechanistic model that involves "unthreading" of either of the longer intercalators **3** or **4** could be produced that fits the dissociation data. Of course, we cannot *rigorously* rule out model **A**. For example, it is possible, albeit unlikely, that the "threading" steps do not produce spectroscopic changes that are detectable by the absorbance techniques used in these kinetic studies. Assuming no such ambiguities exist, we propose a mechanism below for

(32) Bailly, C.; Hamy, F.; Waring, M. J. *Biochemistry* **1996**, *35*, 1150−1161.
(33) Capelle, N.; Barbet, J.; Dessen, P.; Blanquet, S.; Roques, B.; Le Pecq, J.-B. *Biochemistry* **1979**, *17*, 3354−3366.
(34) Fox, K. R.; Waring, M. J. *Biochim. Biophys. Acta* **1984**, *802*, 162−168.
(35) Teitelbaum, H.; Englander, S. W. *J. Mol. Biol*. **1975**, *92*, 93−111.
(36) Teitelbaum, H.; Englander, S. W. *J. Mol. Biol*. **1975**, *92*, 55−78.
(37) Kaiser, E.; Colescott, R. L.; Bossinger, C. D.; Cook, P. I. *Anal. Biochem*. **1970**, *2324*, 595.

the dissociations of **2**−**4** from poly(dAdT) that is consistent with all of the available data if the compounds are bound according to model **B**.

Mechanism of Dissociation. We investigated whether a mechanistic scheme within model **B** could be generated that predicts the similarity in dissociation profiles between the different compounds for a given type of DNA. We began with the assumptions that (a) the elementary steps in a sequential mechanism should be similar among all three of the polyintercalators **2**−**4**, (b) the N-to C-terminal asymmetry of the compounds could be ignored, and that (c) in the presence of SDS, which solvates the unbound chromophores, bimolecular reassociation rates are negligible. These assumptions allowed us to prune the many branching steps that are theoretically possible for a multiintercalating species down to a manageable number. We then evaluated potential mechanisms by comparing the resulting theoretical dissociation curves with the actual data.

Specifically, we constructed theoretical absorbance-vs-time curves assuming a constant increase in absorbance per chromophore expelled from the DNA. A rate equation for the unbound species was generated for a given mechanism and substituted into the absorbance expression (Supporting Information). The resulting differential equation was numerically solved for a given set of rate constants and plotted against the experimental data. The rate constants were manually varied, and the resulting plots were used to obtain an interpolative fit. While this approach may seem rather primitive, the complexity of the resulting analytical solutions prevented the use of a mathematically more rigorous least-squares fit. Plotting the numerical solutions for each set of differential equations, on the other hand, allowed us to evaluate rapidly the viability of a particular mechanism directly using the elementary step rate constants with no restrictions on the complexity of the resulting exponential function.

Initially we attempted to reproduce the dissociation profiles of all three compounds with a simple mechanistic scheme in which the intercalating groups dissociate in no particular order and at approximately the same rate. This model was unable to produce satisfactory fits for any set of experimental data and was quickly abandoned.

In an alternative approach, we introduced as a constraint the fact that the dimer **2** binds cooperatively in units of two (as observed in the DNAse I footprinting experiments.) In such a scenario, the rates of dissociation of the individual intercalating groups are largely dependent upon the occupancy of neighboring sites. To make the math tractable, we postulated a stepwise nonbranching mechanism (Figure 8), based on the following assumptions: First, since cooperativity was observed with the dimer, we inferred that binding to the *third*, but not necessarily to the *fourth*, occupied site is cooperative for each of the compounds. Second, the fact that the K_{eq} for the dimer is less than the square of the K_{eq} of the monomer implied that the binding of *adjacent* groups (separated by two base pairs) is non- or perhaps even anticooperative. In terms of off-rates these data suggested the order $k_{third} < k_{first} \approx k_{second} \approx k_{fourth}$ for the dissociation from the respective intercalated sites.

The best fits (available as Supporting Information) obtained for the dissociation of compounds **2**−**4** from poly(dAdT) according to our model (Figure 8) yielded the rate constants listed in Table 4 (note the similarity in the rate constant sets for the three compounds). However, the postulated mechanistic scheme failed to produce satisfactory fits for the poly(dGdC) data.

The results shown in Table 4 for the poly(dAdT) data support our initial assumptions. Numbers in parentheses indicate

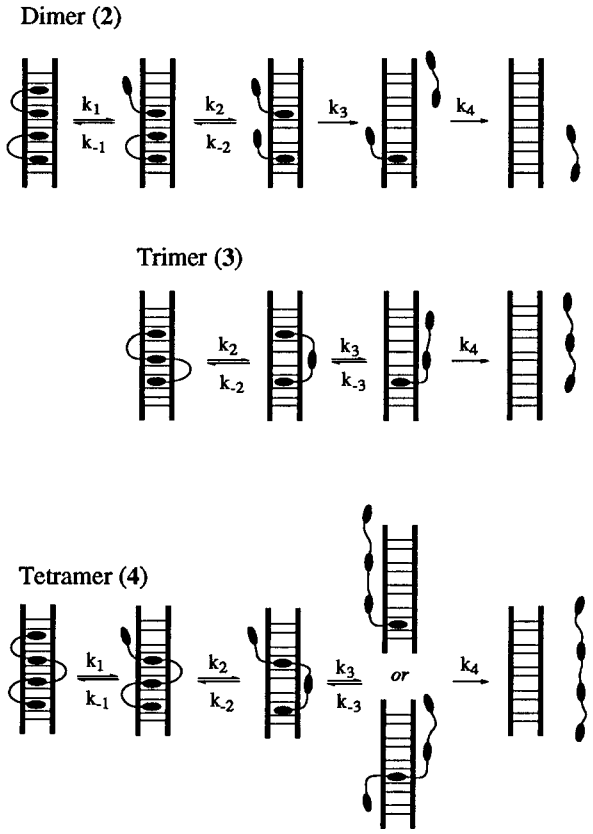

Figure 8. Simplified mechanistic scheme for the dissociation of intercalators **2**−**4** in which the dimer **2** binds cooperatively in pairs. All three compounds dissociate from DNA in a similar stepwise pattern, in which the off-rates depend on the occupancy of neighboring intercalated sites.

"flexible" rate constants whose values could be varied significantly (within an order of magnitude) without a large impact on the fit. These numbers show k_3 to be the rate limiting step, and attempts to reverse the relative size of the constants failed. Note that for the trimer and tetramer the proposed order of dissociation from the intercalated sites would require the existence of intermediates in which dissociated chromophores are tethered on both sides by intercalated groups (Figure 8). However, given the small difference between k_2 and k_3, it is possible that any "middle" bound residue in the trimer and tetramer would be held tightly in position by the linkers on both sides, giving rise to an alternative mode of dissociation (Figure 9, pathway *b*).

Our mathematical model does not explicitly differentiate between intermediates such as *a* and *b* in the dissociation reaction of compound **3**, as the absorbance curve is simulated by simply counting the number of unbound chromophores in each species. For the dimer **2**, where the two corresponding intermediates (Figure 10) theoretically give rise to kinetically distinct pathways, we observed an equally good fit for both mechanisms (via intermediates *c* or *d*, corresponding to *a* and *b* for the trimer, respectively), with the same set of rate constants. This is not surprising considering the negligible reverse rate constants ($k_{-2a} \approx k_{-3b} \approx 0.0005\ s^{-1}$) in both instances. In light of the above, we propose that in reality the dissociation could proceed through a combination of these two pathways. Since each elementary step is virtually irreversible in the poly(dAdT) fits, the constants obtained are possibly linear combinations of the elementary step rate constants.

The existence of such alternate pathways may account for the more complex dissociation curves observed for poly(dGdC). The slower experimental off-rates measured for all three

Table 3. Dissociation Rates

	1		**2**		**3**		**4**	
	k (s^{-1})	A (%)	k (s^{-1})	A (%)	k (s^{-1})	A (%)	k (s^{-1})	A (%)
poly(dAdT)	15.4	27	0.12	8	0.097	12	0.11	7
	6.6	73	0.021	92	0.021	88	0.019	93
poly(dGdC)	0.98	23	5.9×10^{-4}	8	6.9×10^{-4}	6	4.6×10^{-4}	5
	0.047	77	4.6×10^{-5}	15	8.2×10^{-5}	15	3.7×10^{-5}	15
			3.8×10^{-6}	77	4.5×10^{-6}	79	2.3×10^{-6}	80
CT DNA	5.1	24	5.5×10^{-3}	34	6.0×10^{-3}	37	4.3×10^{-3}	39
	1.0	36	5.0×10^{-4}	35	5.5×10^{-4}	35	5.0×10^{-4}	46
	0.23	40	1.0×10^{-4}	31	1.1×10^{-4}	28	8.1×10^{-5}	15

[a] Numbers refer to compounds **1**−**4**. [b] Association and dissociation rate constants determined by fitting the spectrophotometrically-determined decay traces to up to three exponentials (see Experimental Section). [c] Relative amplitudes from curve fits as percentage of total.

Table 4. Rate Constants Obtained from Fitting Dissociation Curves of Compounds **2**−**4** with poly(dAdT) According to Mechanism in Figure 8

	compd		
	2	**3**	**4**
k_1[a]	0.12		0.11
k_{-1}	7×10^{-4}		5×10^{-4}
k_2	7.0×10^{-2}	0.12	7.0×10^{-2}
k_{-2}	(5×10^{-4})[b]	(5×10^{-4})	(5×10^{-4})
k_3	2.1×10^{-2}	2.1×10^{-2}	2.1×10^{-2}
k_{-3}		(5×10^{-4})	(5×10^{-4})
k_4	(0.12)	(0.10)	(0.12)

[a] Rate constants (s^{-1}). [b] Parentheses denote numbers that can be varied by at least an order of magnitude without greatly affecting the closeness of the fit.

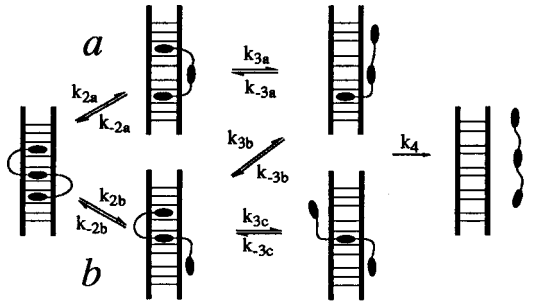

Figure 9. Proposed branching pathways for the dissociation of trimer **3**, according to the calculated rate constants (Table 4). A theoretical model based on hypochromism does not differentiate between pathways *a* and *b*.

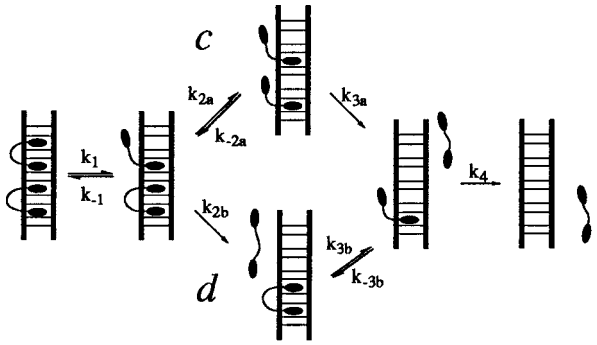

Figure 10. Theoretically distinct pathways in the dissociation of dimer **2**, corresponding to the branching proposed for compounds **3** (Figure 9) and **4** (not shown).

compounds suggest both smaller dissociation and larger reverse (reassociation) constants, which may lead to more complex kinetic behavior, than for poly(dAdT). Furthermore, one or more of the assumptions that allowed a fit of the poly(dAdT) data may not be valid in the case of the dissociations from poly(dGdC). For example, a branching of the mechanistic steps would have to be introduced in order to take into account the N- to C-terminal asymmetry of the polyintercalators, a factor that may be important on the much slower time scale of the poly(dGdC) dissociations. In order to take this branching into account, many more kinetic constants would have to be introduced, which seriously limits the credibility of any deduced model. Finally, it may be that **2**−**4** adopt a somewhat different mode of binding to poly(dGdC) compared with poly(dAdT).

Conclusion

We have described a new class of polyintercalating compounds and the first known tetraintercalator. Using DNAse I footprinting, we found that cooperativity is an important feature in the binding of our polyintercalators to double-stranded DNA. Using kinetic data obtained from stopped-flow and manual mixing techniques, we were able to propose a mode of binding for compounds **2**−**4** and a mechanism for their dissociations from poly(dAdT). The solid phase synthesis of these compounds, in which the intercalating groups are attached to one another by peptide linkers, suggests the possibility of developing novel DNA-binding compounds using the rapidly advancing techniques of combinatorial and solid phase chemistry. With this design we may also tap into the burgeoning field of non-peptide solid-phase synthesis to generate polyintercalators separated by rigid, highly functionalized linkers in which properties such as sequence specificity or enzyme inhibition (i.e., topoisomerase inhibition) could be selected from a library or rationally designed.

Experimental Section

General Considerations. Routine NMR spectra were recorded on a Bruker 250 MHz. Spectra of compounds **2**−**4** were recorded on a Varian 500 MHz instrument. Solvents and starting materials were used without further purification unless otherwise stated. Organic chemicals were obtained from Aldrich and nucleic acids were obtained from Sigma. Dissociation profiles were simulated in Mathematica 2.2 (Wolfram Research) on a UNIX Sun SPARC 2000 station.

***N*-(2-*tert*-Butoxycarbonylaminoethyl)-*N*′-(2-carboxyethyl)-1,4,5,8-naphthalenetetracarboxylic Diimide.** 1,4,5,8-Naphthalenetetracarboxylic dianhydride (8.96 g, 33.4 mmol) was suspended in 450 mL of *i*-PrOH. Mono-*tert*-butoxycarbonylaminoethylamine (5.34 g, 33.4 mmol) and β-alanine benzyl ester *p*-toluenesulfonate salt (11.72 g, 33.4 mmol) were added to the mixture, followed by *N*,*N*-diisopropylethylamine (6.4 mL, 37 mmol). The mixture was heated to reflux for 24 h, after which it was concentrated *in vacuo*. The resulting solid was partitioned between CH_2Cl_2 (450 mL) and 0.1 M sodium citrate buffer (pH 4.5, 500 mL). The organic layer was washed with citrate buffer (2×100 mL), saturated $NaHCO_3$ (3×100 mL), and then brine (100 mL) and dried over anhydrous $NaSO_4$. MeOH (100 mL) was added to the mixture, and it was filtered through a short pad of silica gel. The filter was rinsed with 10% MeOH/CH_2Cl_2 (100 mL), and the supernatant concentrated to yield the expected statistical mixture of products (18.7 g, 91%). This mixture was carried on to the next step without further purification.

The above tan solid was suspended with sonication in absolute EtOH (250 mL) and purged with Ar. Pd/C (14 g, 10%) was added, followed by 15 mL of 1,4-cyclohexadiene added dropwise. The mixture was charged with H_2 at atmospheric pressure and stirred for 48 h. After concentrating the reaction to 50 mL (bath temperature 30 °C, 20 Torr), 250 mL of 15% TEA/CH_2Cl_2 was added. The resulting slurry was stirred for 20 min and filtered through Celite. The filter was rinsed with 10% TEA/CH_2Cl_2 until the rinsings were colorless, and the solution was evaporated *in vacuo*. The resulting solid was taken up into CH_2Cl_2 with just enough MeOH to allow for complete solvation, and the product mixture was deposited onto silica by evaporation. Chromatographic separation using a gradient of 0 → 10% MeOH in 10% TEA/CH_2Cl_2 yielded the TEA salt of the BOC-protected amino acid as the second, bright orange band. After concentration the solid was taken up into 10% MeOH/CH_2Cl_2 and 20 mL of HOAc was added. Hexanes (300 mL) were slowly added to precipitate the product. After cooling for several hours, the mixture was filtered, and the precipitate was rinsed with MeOH and dried *in vacuo* to yield the carboxylic acid (5.10 g, 27%) as a fine white powder: ^{1}H NMR (DMSO-d_6) δ 8.58 (s, 4H), 6.90 (br t, 1H), 4.25 (t, J = 7.5 Hz, 2H), 4.12 (br t, 2H), 3.27 (br q, 2H), 2.62 (t, J = 7.4 Hz, 2H), 1.20 (s, 9H); ^{13}C NMR (DMSO-d_6) δ 172.4, 162.7, 162.4, 155.8, 130.4, 130.3, 126.4, 126.1, 77.5, 37.6, 36.1, 32.0, 28.1; HRMS (FAB) *m*/*z* 482.1547 (482.1563 calcd for $C_{24}H_{24}N_3O_8$).

***N*-2-(*N*$^{\alpha}$-9-Fluorenylmethoxycarbonylglycyl)aminoethyl-*N*′-(2-carboxyethyl)-1,4,5,8-naphthalenetetracarboxylic Diimide.** The above BOC-protected amino acid (2 g, 4.16 mmol) was suspended in 15 mL of CH_2Cl_2, and 15 mL of TFA was added slowly. After standing for 10 min the solution was evaporated, and the residual TFA removed by azeotropic evaporation (2×) from heptane. The resulting solid was triturated with ether, filtered, and dried *in vacuo*. The solid was suspended in DMF (15 mL), and *N*-9-fluorenylmethoxycarbonylglycine pentafluorophenyl ester (1.92 g, 4.16 mmol) was added, followed by 1-hydroxybenzotriazole (HOBT, 561 mg, 4.16 mmol) and 2,6-lutidine (890 mg, 8.32 mmol). After stirring for 4 h the mixture was poured slowly into rapidly stirred H_2O (150 mL), and the resulting suspension was allowed to stand for several hours. The mixture was filtered, and the resulting yellow solid was rinsed with H_2O and dried in the presence of P_2O_5 in a vacuum desiccator overnight. The crude product was triturated with Et_2O several times (to remove the residual 1-hydroxybenztriazole and pentafluorophenol), filtered, and dried *in vacuo* to yield the fully protected glycine adduct (86%) as a yellow powder. ^{1}H NMR (300 MHz, DMF-d_7) δ 8.66 (s, 4H), 8.12 (t, 1H, J = 5.7 Hz), 7.88 (d, 2H, J = 7.4 Hz), 7.68 (d, 2H, J = 7.3 Hz), 7.4 (m, 1H), 7.42 (t, 2H, J = 7.4 Hz), 7.30 (t, 2H, J = 7.3 Hz), 4.40 (t, 2H, J = 7.3 Hz), 4.31 (t, 2H, J = 5.6 Hz), 4.20 (d, 2H, J = 6.9 Hz), 4.11 (t, 1H, J = 6.5 Hz), 3.75 (d, 2H, J = 5.8 Hz), 3.66 (br dt, 2H, J_1 = 5.5), 2.81 (t, 2H, J = 7.7 Hz); ^{13}C NMR (300 MHz, DMF-d_7) δ 173.0, 170.4, 163.6, 162.9, 157.3, 144.8, 141.6, 131.1, 131.0, 128.3, 127.7, 127.2, 127.0, 126.0, 120.6, 67.0, 47.5, 44.6, 40.6, 37.0, 36.2, 32.5; HRMS (FAB) 661.1934 (661.1934 calcd for $C_{36}H_{29}N_4O_9$, $M^+ + H$).

***N*-2-(*N*$^{\alpha}$-9-Fluorenylmethoxycarbonylglycyl)aminoethyl-*N*′-(2-pentafluorophenoxycarbonylethyl)-1,4,5,8-naphthalenetetracarboxylic Diimide (5).** The above carboxylic acid (1.11 g, 1.68 mmol) was dissolved in dry DMF (5 mL) and pentafluorophenol (335 mg, 1.85 mmol), followed by dicyclohexylcarbodiimide (381 mg, 1.85 mmol), were added. After stirring for 16 h the reaction was evaporated *in vacuo* at room temperature to a viscous sludge, to which was added dry dioxane (10 mL). The resulting suspension was stirred for 5 h and then filtered. The bright yellow filtrate was evaporated *in vacuo*, and the resulting solid was triturated with pentane. The mixture was filtered, and the product was rinsed with pentane and dried *in vacuo* to yield the pentafluorophenyl ester (1.21 g, 1.47 mmol, 87%) as a yellow powder. ^{1}H NMR (300 MHz, DMF-d_7) δ 8.67 (s, 4H), 8.13 (t, 1H, J = 5.6 Hz), 7.86 (d, 2H, J = 7.4 Hz), 7.65 (d, 2H, J = 7.3 Hz), 7.47 (t, 1H, J = 6.0 Hz), 7.39 (t, 2H, J = 7.3 Hz), 7.27 (t, 2H, J = 7.4 Hz), 4.55 (t, 2H, J = 7.1 Hz), 4.30 (t, 2H, J = 5.6 Hz), 4.16 (d, 2H, J = 6.8 Hz), 4.09 (d, 1H, J = 6.4 Hz), 3.72 (d, 2H, J = 5.9 Hz), 3.63 (dt, J = 6.1 Hz), 3.35 (t, 2H, J = 7.2 Hz); ^{13}C NMR (300 MHz, DMF-d_7) δ 170.4, 168.4, 163.6, 162.9, 157.3, 144.8, 141.6, 131.1, 128.3, 127.7, 127.4, 127.1, 127.0, 126.9, 126.0, 67.0, 47.5, 44.6, 40.7, 37.6, 36.3, 34.3; HRMS (FAB) 827.1775 (827.1776 calcd for $C_{42}H_{28}N_4O_9F_5$, $M^+ + H$).

***N*$^{\alpha}$-9-Fluorenylmethoxycarbonyl-(*N*$^{\epsilon}$-*tert*-butoxycarbonyl)lysylglycylglycine.** *N*-9-Fluorenylmethoxycarbonyl-(*N*$^{\epsilon}$-*tert*-butoxycarbonyl)lysine (0.9 g, 1.92 mmol) was dissolved, with *N*-hydroxysulfosuccinimide (458 mg, 2.11 mmol), in 5 mL of 10% H_2O/DMF. 1-Ethyl-3-[3-dimethylaminopropyl]carbodiimide hydrochloride (EDC) (405 mg, 2.11 mmol) was added, and the mixture was stirred for 4 h. The triethylammonium salt of diglycine (492 mg, 2.11 mmol.) (It was prepared as follows: Diglycine was dissolved in water, and excess triethylamine was added. EtOH was added until the solution became homogeneous, and the solution was evaporated to dryness *in vacuo*. The resulting solid was suspended in MeOH, filtered, rinsed with Et_2O, and dried *in vacuo*.) was dissolved in 5 mL of H_2O and added dropwise to the reaction mixture. After stirring for 16 h the reaction mixture was partitioned between EtOAc and Na citrate buffer (0.2 M, pH 4.5). The aqueous phase was extracted with EtOAc (3 × 25 mL), and the combined organic layers were dried over anhydrous Na_2SO_4, filtered, and concentrated *in vacuo*. The resulting white foam was purified by chromatography on silica gel with 5% MeOH/CH_2Cl_2. Crystallization by the slow addition of pentane to a solution of the product in 10% EtOAc/CH_2Cl_2 (25 mL) yielded FMOCN-Lys(ϵ-BOC)-Gly-Gly-OH as a white powder (735 mg, 69%). ^{1}H NMR (300 MHz, DMSO-d_6) δ 8.17 (t, 1H, J = 5.4 Hz), 8.09 (t, 1H, J = 5.8 Hz) 7.87 (d, 2H, J = 7.4 Hz), 7.72 (dd, 2H, J = 7.2, 4.3 Hz), 7.53 (d, 1H, J = 7.8 Hz), 7.41 (t, 2H, J = 6.9 Hz), 7.32 (t, 2H, J = 7.0 Hz), 6.76 (t, 1H, J = 5.3 Hz), 4.32−4.19 (m, 3H), 3.96 (br q, 1H), 3.74 (t, 4H, J = 6.1 Hz), 2.88 (q, 2H, J = 4.5 Hz), 1.7−1.1 (c, 6H), 1.35 (s, 9H); ^{13}C NMR (300 MHz, DMSO-d_6) δ 172.3, 171.1, 169.1, 156.1, 155.6, 143.9, 143.8, 140.7, 127.6, 127.1, 125.3, 120.1, 77.3, 65.6, 54.7, 46.7, 40.6, 39.7, 31.4, 29.2, 28.3, 22.8; HRMS (FAB) *m*/*z* 583.2793 (583.2768 calcd for $C_{30}H_{39}N_4O_8$, $M^+ + H$).

***N*$^{\alpha}$-9-Fluorenylmethoxycarbonyl-(*N*$^{\epsilon}$-*tert*-butoxycarbonyl)lysylglycylglycine Pentafluorophenyl Ester (6).** The above carboxylic acid (735 mg, 1.26 mmol) was dissolved in dry dioxane (6 mL) and pentafluorophenol (349 mg, 1.89 mmol) followed by dicyclohexylcarbodiimide (DCC, 285 mg, 1.39 mmol) was added. After stirring for 5 h, the reaction was filtered, the precipitate was rinsed with dry dioxane (5 mL), and the solution was evaporated *in vacuo*. The resulting solid was triturated with hexanes, filtered, and dried *in vacuo* to yield the pentafluorophenyl ester (803 mg, 1.07 mmol, 85%) as a white crystalline solid. ^{1}H NMR (300 MHz, CD_2Cl_2) δ 7.75 (d, 2H, J = 7.4 Hz), 7.58 (d, 2H, J = 7.4 Hz) 7.44 (br m, 1H), 7.39 (t, 2H, J = 7.2 Hz), 7.28 (t, 2H, J = 7.4 Hz), 7.06 (br m, 1H), 5.96 (br m, 1H), 4.81 (br m, 1H), 4.38 (d, 2H, J = 7.1 Hz), 4.29 (d, 2H, J = 5.9 Hz), 4.19 (t, 1H, J = 6.7 Hz), 4.05 (br t, 1H), 3.97 (d, 2H, J = 5.6 Hz), 3.06 (br dt, 2H), 1.95−1.3 (c, 6H) 1.30 (s, 9H); ^{13}C NMR (300 MHz, DMSO-d_6) δ 172.4, 169.8, 166.6, 156.1, 155.6, 143.9, 143.8, 140.7, 127.6, 127.0, 125.3, 120.0, 77.3, 65.7, 54.7, 46.7, 41.7, 32.9, 31.4, 29.2, 28.8, 22.8; HRMS (FAB) *m*/*z* 749.2579 (749.2610 calcd for $C_{36}H_{38}N_4O_8F_5$, $M^+ + H$).

General Procedure for the Solid Phase Synthesis of Compounds 1−4. Lysine-functionalized 2-chlorotrityl polystyrene resin (Advanced Chemtech, 335 mg, ∼0.31 mmol/g loading) was added to a 10 mL fritted-glass filter flask equipped with a screw cap and Teflon stopcock. The resin was shaken for a few minutes with 50% Et_2N/DMF (5 mL) and then rinsed with DMF (3 × 5 mL), *i*-PrOH (3 × 5 mL), and then DMF (3 × 5 mL). The resin was suspended in 2 mL of DMF, and **5** (212 mg, 0.26 mmol) was added. HOBT (35 mg, 0.26 mmol) was added, and the mixture was shaken for 3 h using a simple oscillating shaker. (Completion of the coupling could not be monitored using the Kaiser test[37] because compounds containing the 1,4,5,8-tetracarboxylic diimide moiety consistently gave a false positive reaction. The use of a 3 h coupling time and 2.5 equiv of the pentafluorophenyl esters, however, generally gave high coupling yields based on analysis of the final products.) The resin was rinsed (DMF/*i*-PrOH/DMF) and treated with 50% Et_2N/DMF for 30 min. The resin was rinsed again (DMF/*i*-PrOH/DMF), and then FMOC-Lys(ϵ-BOC)-Gly-Gly-OPfp **6** (193 mg, 0.26 mmol) was added along with HOBT (35 mg, 0.26 mmol). After shaking for 3 h the resin was rinsed, deprotected, and rinsed again as described above. The process was repeated until the desired number of units had been coupled. After the final deprotection step the resin was treated with 1:1:3 HOAc/2,2,2-trichloroethanol/CH_2Cl_2 (7 mL) for 1 h. The resin was filtered using

a cintered glass funnel, and the supernatant was evaporated to yield an olive green solid. To ensure that all of the compound had been cleaved, the resin was treated with 5% TFA/CH_2Cl_2 for 10 min and filtered. The filtrate was evaporated *in vacuo* to yield an orange oil and combined with the original material that had been cleaved from the resin. To this mixture was added 1:1 TFA/CH_2Cl_2 (10 mL), and, after 10 min, the solution was evaporated *in vacuo*. The resulting solid was evaporated from heptane (2 × 10 mL), taken up in H_2O (20 mL), and filtered through a 0.45 m nylon syringe filter. The solution was loaded onto a reversed phase C_{18} column (PepRPC 15 m, Pharmacia) and eluted with a gradient of 10 mM TFA/H_2O → 0.8% TFA/CH_3CN over 180 min with a flow rate of 0.75 mL/min. The main fraction was collected and determined to be homogeneous by HPLC (C_{18}, same conditions as above). The product fractions were pooled and lyophilized to yield **21**, **22**, **23**, or **24** as a light green solid, with yields in the range of 25−35% based on the initial loading of the resin.

Compound 1. ^{1}H NMR (500 MHz, 10% D_2O/H_2O) δ 8.64 (d, 2H, J = 7.6 Hz), 8.59 (d, 2H, J = 7.6 Hz), 8.33 (t, 1H, J = 5.8 Hz), 8.27 (d, 1H, J = 7.5 Hz), 4.41 (m, 2H), 4.32 (t, 2H, J = 5.9 Hz), 4.23 (dt, 1H, J = 5.2, 7.9 Hz), 3.71 (s, 2H), 3.64 (dt, 2H, J = 5.9, 5.8 Hz), 2.92 (br m, 2H), 2.72 (t, 2H, J = 6.8 Hz) 1.72 (m, 2H), 1.61 (m, 2H), 1.34 (p, 2H, J = 7.6); HRMS (FAB) *m*/*z* 567.2222 (567.2203 calcd for $C_{27}H_{31}N_6O_8$, M^+).

Compound 2. ^{1}H NMR (500 MHz, D_2O) δ 8.41−8.32 (m, 8H), 4.48−4.29 (m, 5H), 4.25 (t, 2H, J = 8.9 Hz), 4.20 (t, 2H, J = 9.0 Hz), 4.11−3.83 (m, 6H), 3.74 (s, 2H), 3.59 (m, 4H), 3.03 (t, 2H, J = 7.7 Hz), 2.93 (t, 2H, J = 7.6 Hz), 2.86 (m, 2H), 2.71 (t, 2H, J = 7.1 Hz), 1.94−1.3 (m, 12H); HRMS (FAB) *m*/*z* 1229.4638 (1229.4652 calcd for $C_{89}H_{101}N_{22}O_{26}$, $M^+ - H$).

Compound 3. ^{1}H NMR (500 MHz, D_2O) δ 8.43−8.22 (m, 12H), 4.32−4.11 (m, 15H), 3.99−3.82 (m, 12H), 3.77 (s, 2H), 3.68 (m, 6H), 3.01 (t, 4H, J = 7.5 Hz), 2.94 (t, 2H, J = 7.6 Hz), 2.77 (m, 4H), 2.66 (t, 2H, J = 7.2 Hz), 1.90−1.29 (m, 18H); HRMS (FAB) *m*/*z* 1891.7175 (1891.7101 calcd for $C_{89}H_{101}N_{22}O_{26}$, $M^+ - 2H$).

Compound 4. ^{1}H NMR (500 MHz, D_2O) δ 8.4−8.1 (m, 16H), 4.38−4.1 (m, 20H), 3.98−3.70 (m, 18H), 3.77 (s, 2H), 3.55 (m, 8H), 3.02 (t, 6H, J = 7.5 Hz), 2.96 (t, 2H, J = 7.5 Hz), 2.75 (m, 6H), 2.66 (t, 2H, J = 7.3 Hz), 1.90−1.3 (m, 24H); MS (FAB) *m*/*z* 2554 (2554 calcd for $C_{120}H_{136}N_{30}O_{35}$, $M^+ - 4H$).

Unwinding Angles. The unwinding angles for compounds **1**−**4** were determined with a Cannon−Ubblehode dilution viscometer (size 75) by the method of Revét et al.[31] Flow times were measured in triplicate with a hand-held digital stopwatch; the average deviation of a set of measurements was 0.5−0.7 s or 0.5%. The 11 kilobase-pair plasmid pMC1403, a donation of professor Ian Molineux at the University of Texas, was amplified in *E. coli* DH5α cells and purified by CsCl density gradient centrifugation in the presence of propidium iodide. All unwinding experiments were performed in TE buffer with 50 mM NaCl at pH 7.5. The slope of the Vinograd plot for ethidium bromide was considered to represent an unwinding angle of 26°. To determine the unwinding angle of compound **1**, the slope of its Vinograd plot was compared with that of ethidium bromide. For compounds **2**−**4**, titrations performed at multiple DNA concentrations, from 0.15 to 0.25 mM, gave identical unwinding equivalence points, confirming that these compounds are completely bound at these concentrations.

DNA Lengthening. Titrations were performed with the viscometric technique described above, and the data were treated by the method of Cohen and Eisenberg.[30] Calf thymus DNA (Sigma, Type XV) was sonicated in a low power sonicator on ice for 1.5 h, filtered through a 0.45 micron nylon filter, and dialyzed against TE buffer with 50 mM NaCl using 10 000 MWCO dialysis tubing. The DNA concentration was 0.1 mM base pairs. As determined in the supercoiled DNA unwinding experiments and in titrations with excess CT DNA, compounds **2**−**4** were completely bound to the DNA at the concentrations studied; therefore, lengthening data for these compounds was not corrected for binding constant effects. For monomer **1**, a binding constant of 1.0×10^5 (*vide infra*) was used to calculate the value *r* for each titration.

Equilibrium Constant. A stock solution of sonicated calf thymus DNA (1.5 mM base pairs in TE buffer with 50 mM NaCl) was added via syringe in increments to a solution of **1** (7.2 μM in the same buffer). The decrease in the monomer's absorption at 386 nm due to intercalation was measured using a Hewlett-Packard 8452A diode array spectrophotometer. The data were converted into Scatchard form using 10 375 M^{-1} cm^{-1} as the molar extinction coefficient for bound **1**, derived from a Beer's Law titration of **1** into a 1.5 mM solution of CT DNA. To derive values for K_a and *n*, the data were fit to the McGee−von Hippel[28] equation using the KaleidaGraph curve fitting routine.

Stopped-Flow Kinetics. Experiments were performed using a Dionex D-130 stopped-flow apparatus with a 20 mm pathlength. The monochromator was set at 386 nm, and the signal from the photomultiplier was amplified with a digital oscilloscope. All experiments were performed at 25 °C in 10 mM Na PIPES buffer at pH 7.0 with 50 mM NaCl (PIPES 05E). For the association experiments, solutions of **1**−**4** at concentrations of 10, 13.3, 20, and 40 μM, respectively, were mixed upon actuation with equal volumes of CT DNA, poly-dAdT, and poly-dGdC, at concentrations of 0.2, 0.15, and 0.15 mM, respectively. For the dissociation experiments, the solutions resulting from the association experiments were collected and mixed upon actuation with equal volumes of 4% SDS. For compounds **2**−**4**, little or no dissociation was observed from any of the DNAs over a 50 s time interval, indicating that direct mixing could be used to observe all components of their dissociation kinetics. All kinetic traces and residuals representing the best up to three exponentials are available as Supporting Information.

Slow Dissociation. In a typical experiment, 0.5 mL of a 4% SDS solution in PIPES 05E was mixed with 0.5 mL of a solution of DNA−ligand complex in a quartz cuvette of 10 mm pathlength, taking care to avoid trapping air bubbles along the walls of the cuvette. Initial ligand concentrations were the same as those used in the stopped flow experiments, and initial concentrations of DNA were at 0.2 mM for CT DNA, poly(dAdT), and poly(dGdC). Within 20 s of mixing, the absorbance at 386 nm was recorded as a function of time using a Hewlett-Packard 8452A spectrophotometer.

DNAse I Footprinting. T4 polynucleotide kinase, DNAse I, and [γ-^{32}P]ATP were purchased from Amersham. Electrophoretic reagents were purchased from J. T. Baker, Inc. The 78-mer DNA was synthesized on an Applied Biosystems 381A DNA synthesizer using the phosphoramidite method. The oligonucleotides were cleaved from the column material by concentrated ammonium hydroxide and deprotected overnight at 55 °C. The single stranded DNA fragments were purified by a 12% preparative denaturing polyacrylamide gel. Purified oligonucleotides were 5′-labeled with [γ-^{32}P]ATP and T4 polynucleotide kinase and annealed with their complementary strands to make duplex DNA. The labeled duplex DNA was purified using native 8% PAGE.

The 5′-^{32}P-labeled 78-mer DNA (500 nM base pairs) was incubated with various concentrations of compounds **1**−**4** for 30 min at room temperature in 20 μL of a solution containing 20 mM sodium phosphate (pH 7.5) and 2 mM $MgCl_2$. Then 0.1 U of DNAse I was added to the reaction mixture and incubated for 1 min. The reaction was quenched by addition of 180 μL solution containing 3 mM EDTA, 0.3 M sodium acetate, and 5 μg tRNA. The cleaved DNA was ethanol precipitated and loaded onto a 12% denaturing sequencing gel. The gels were exposed on X-ray film and/or phosphorimager screens and analyzed by ImageQuaNT 4.1 software from Molecular Dynamics.

Acknowledgment. This material is based in part upon work supported by the Texas Advanced Research Program under Grant No. ARP-147 and the Welch Foundation (Grant F-1188). We would also like to thank Ms. Jessica Hernandez for synthetic and analytical help.

Supporting Information Available: Stopped flow association and dissociation kinetic traces of compounds **1**−**4**, absorbance spectrum of tetramer **4**; UV dissociation profiles of compounds **2**−**4**, and description of calculational methods (11 pages). See any current masthead page for ordering and Internet access instructions.

JA9706108